Chemical Engineering Journal 354 (2018) 85–92

Contents lists available at ScienceDirect

Chemical Engineering Journal

journal homepage: www.elsevier.com/locate/cej

The influence of low-temperature hydration methods on the stability of Cu-SAPO-34 SCR catalyst

Yi Cao[a], Dong Fan[a], Peng Tian[a,*], Lei Cao[a], Tantan Sun[a,b], Shutao Xu[a], Miao Yang[a], Zhongmin Liu[a,*]

[a] National Engineering Laboratory for Methanol to Olefins, Dalian National Laboratory for Clean Energy, Dalian Institute of Chemical Physics, Chinese Academy of Sciences, Dalian 116023, PR China
[b] University of Chinese Academy of Sciences, Beijing 100049, PR China

HIGHLIGHTS

- Cycle hydration is firstly proposed to explore the stability of Cu-SAPO-34.
- The texture and structure of Cu-SAPO-34 keep well after hydration treatment.
- $Si(OAl)_4$ transfer into Si islands, causing the loss of Brönsted acid sites.
- Cycle treatment causes an obvious variation in the redox ability of Cu species.

GRAPHICAL ABSTRACT

The severe activity loss of the catalysts after multiple-cycle hydration treatment is revealed to be caused by the combined effect of the decrease of strong acid sites and the variation of the reducibility of Cu^{2+} ions, and the decrease of strong acid sites is caused by the transformation of iso-$Si(OAl)_4$ species in to Si islands.

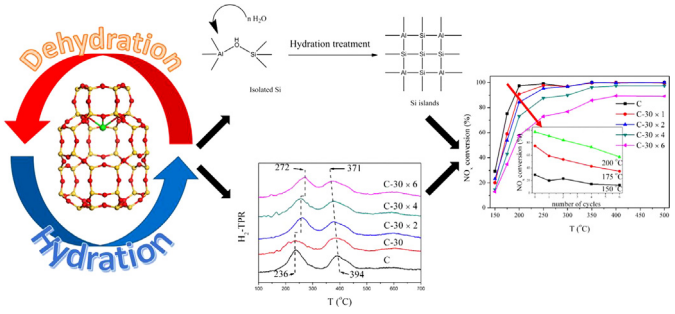

ARTICLE INFO

Keywords:
Cu-SAPO-34
Hydrothermal stability
Deactivation
Cycle hydration
NH_3-SCR

ABSTRACT

Low-temperature hydration experiments are designed to explore the influence of hydration time and cycle hydration on the stability of Cu-SAPO-34 catalyst. All the hydration treatments are conducted at 80 °C. Experiments on the impact of hydration time reveal that a fast activity loss for Cu-SAPO-34 occurs at the initial hydration stage of 30 min, and further extending the time until 24 h only leads to a much slower drop rate. Conversely, cycle hydration, which is close to the working conditions of the SCR catalyst, causes a continuous activity drop as the increase of hydration cycles (steaming for 30 min/cycle). Multiple characterizations reveal that in comparison with hydration time method, cycle hydration induces a faster loss of acid sites and decrease of reducibility of isolated Cu^{2+} to Cu^{+}, both of which cause the severer deactivation of the catalyst. This occurs due to the repeated high-temperature treatments involved in the cycle hydration treatment, which promote the migration of Cu ions among the CHA cages, cause a fast deterioration of Brönsted acid sites, and thus obviously alter the micro-environments of Cu ions and their reducibility.

* Corresponding authors.
E-mail addresses: tianpeng@dicp.ac.cn (P. Tian), liuzm@dicp.ac.cn (Z. Liu).

https://doi.org/10.1016/j.cej.2018.07.195
Received 25 May 2018; Received in revised form 9 July 2018; Accepted 29 July 2018
Available online 30 July 2018
1385-8947/ © 2018 Elsevier B.V. All rights reserved.

1. Introduction

Diesel vehicle has attracted much attention due to its low CO_2 emission, high fuel economy and great power output. However, NO_x emitted from diesel engine causes serious environmental issues, such as photochemical fog, ozone depletion, acid rain and haze [1,2]. In the past decades, selective catalytic reduction of NO_x by NH_3 (NH_3-SCR) technology has been recognized as one of the most efficient ways to eliminate the NO_x in lean burn condition [2,3]. To meet increasingly stringent emission standards, a typical after-treatment system which comprises of diesel oxidation catalyst (DOC), diesel particle filter (DPF) and SCR catalyst is applied [4]. The SCR catalyst would encounter high temperature (> 600 °C, occasionally exceeding 800 °C) with the presence of moisture during the periodic regeneration of DPF [5], and thus, excellent hydrothermal stability is an essential property of the SCR catalyst. Recently, Cu^{2+} ions modified zeolite with the CHA structure (SAPO-34 and SSZ-13) receives much attention due to its great NH_3-SCR performance, high N_2 selectivity, outstanding hydrocarbon resistance and excellent hydrothermal stability [6–9].

Recently, the groups of Li [10,11] and Epling [12] have explored the effect of high temperature vapor on the Cu-CHA catalyst and the discrepancy between Cu-SAPO-34 and Cu-SSZ-13 catalyst. These researches evidence the superior high-temperature hydrothermal stability of Cu-SAPO-34 catalyst and imply its potential application in diesel after-treatment system. However, one weakness associated with SAPO-34 is its sensibility to low-temperature vapor. Brined *et al.* proposed that the low temperature hydrothermal stability of H-SAPO-34 was affected by the quantity of Si-OH-Al bonds and the Si coordination environments [13]. And the hydrolysis of Si-OH-Al bond caused the crystallinity loss of H-SAPO-34. In addition, Buchholz *et al.* revealed that the hydrolysis of H-SAPO-34 comprised of two steps, *i.e.* the hydration of Si-OH-Al bonds and the subsequent coordination of water molecules to Al atoms [14]. The drawback of its low-temperature hydrothermal stability would limit the application of SAPO-34 support in De-NO_x field, since the catalyst might inevitably encounter low-temperature vapor during cold-start period or after turning off the diesel engine.

Recently, some researchers investigated the effect of low temperature vapor on Cu-SAPO-34 catalyst [15–18]. Leistner and Olsson found that the NO_x conversion of Cu-SAPO-34 at 200 °C decreased from the initial value of 87% to 6% after hydration treatment [15]. According to their results, little change occurred in the textural, structural and acidic properties of Cu-SAPO-34 catalyst, and the deactivation of Cu-SAPO-34 catalyst was caused by the loss of active copper species during low-temperature hydration process. In addition, Wang *et al.* reported a similar experimental phenomenon that the NH_3-SCR-rates on Cu-SAPO-34 catalyst with low copper loadings declined drastically after hydration treatment [16]. However, according to them, instead of the loss of the active sites, the deactivation of Cu-SAPO-34 catalyst was mainly attributed to the destruction of the skeleton and the reduction of acid sites. The authors also proposed that isolated Cu^{2+} ions protected the acidic Si-OH-Al bonds and improved the low-temperature hydrothermal stability of Cu-SAPO-34 catalyst. The above reports with somehow controversial conclusions imply that the effect of low-temperature hydration treatment on Cu-SAPO-34 catalyst deserves further investigation. Moreover, a systemic investigation of the effect of the hydration temperature and duration on the low-temperature stability of Cu-SAPO-34 is still missing.

On the other hand, the SCR catalysts must undergo multiple adsorption-desorption cycles of low-temperature vapor during practical application. To the best of our knowledge, few studies have investigated the effect of cycle hydration on the catalytic and physiochemical properties of Cu-SAPO-34 catalyst, although cycle hydration treatment is much close to the practical working conditions of the catalysts. Possibly, the multiple-cycle hydration treatment, which includes the high temperature dehydration process, can exert different influence on the catalysts than simply prolonging the hydration time. Therefore, the data from multiple-cycle hydration may be more reasonable/convincing for judging the long-term durability of the Cu-SAPO-34 catalysts.

Herein, we designed hydration experiments to explore the sensibility of Cu-SAPO-34 SCR catalyst to the low-temperature vapor. The effect of hydration duration and multiple-cycle treatment is systematically investigated. Multiple characterizations are utilized to reveal the variation of the catalysts upon the hydration treatment and the discrepancy among the catalysts from different treatment methods.

2. Materials and methods

2.1. Catalyst preparation and hydration treatment conditions

SAPO-34 was synthesized by hydrothermal method from a gel with molar composition of 2.0 diethylamine (DEA): 0.4 SiO_2: 1.0 Al_2O_3: 1.0 P_2O_5: 50 H_2O. Firstly, 17.94 g of H_3PO_4 (Tianjin Kemiou Chemical Reagent Company) was mixed with 40 g of deionized water, then 11.40 g of pseudobeohmite (68.6 wt% Al_2O_3, Fushun Petroleum No. 3 Factory) was added into the H_3PO_4 solution, and the mixture was stirred for 3 h. After that 1.87 g of fumed silica (Shenyang Huagong Company) and 27.85 g of H_2O was added into the above mixture and stirred for 3 h. After further addition of 11.38 g of DEA (Tianjin Damao Chemical Reagent Company), the mixture was stirred for 24 h to obtain a homogeneous gel, which was then transferred to 150 mL autoclave and heated at 200 °C for 24 h. After crystallization, the product was recovered by filtration, washed with distilled water and dried in air at 120 °C for 24 h. The molar composition of SAPO-34 was $Si_{0.121}Al_{0.493}P_{0.386}O_2$ (determined by XRF).

Cu-SAPO-34 catalyst was prepared by a direct-ion-exchange method recently reported by us [19]. 10 g of as-synthesized SAPO-34 was added into 200 g of 0.01 M $Cu(CH_3COO)_2$ solution, and the suspension was stirred at 50 °C for 5 h. It was then filtered and washed with deionized water. After that, the paste was dried at 110 °C for 12 h and calcined at 600 °C for 3 h to obtain Cu-SAPO-34 catalyst. The final copper loading was 1.14 wt% (measured by XRF), and the fresh catalyst was denoted as C.

Two sets of hydration experiments were performed. One set was to investigate the effect of hydration time on the stability of Cu-SAPO-34 catalyst (named as hydration time method). Firstly, the catalyst was treated with 10% H_2O/N_2 (253.4 mL/min) at 80 °C for 10, 30, 360 and 1440 min, respectively. To avoid the influence of the adsorbed H_2O molecule, the treated catalysts were subsequently heated to 600 °C in dry airflow immediately after hydration treatment. The aged catalysts in this set were denoted as C-X (X representing hydration time). Another set was designed to investigate the effect of multiple-cycle hydration on the stability of Cu-SAPO-34 catalyst (named as cycle hydration method). In one treatment cycle, the catalysts were sequentially treated under 10% H_2O/N_2 (253.4 mL/min) at 80 °C for 30 min, heated to 600 °C in dry air and cooled down to the temperature of 80 °C. The aged catalysts were denoted as C-30 × X (X representing the number of cycles). Detailed procedures about the aging methods are listed in Table 1.

2.2. Catalytic activity test

The catalytic activity measurement was performed by 60 mg of pellets Cu-SAPO-34 catalyst (60–80 mesh) mixed with 240 mg of quartz beads (60–80 mesh) in a fixed bed quartz flow reactor, and the thermal-couple was placed in the center of catalyst bed to determine the temperature of catalyst. Reactant gases were regulated by means of mass-flow controllers (Brookers) before entering the reactor. All gas lines were heated to 100 °C to avoid the condensation of vapor. The concentrations of the simulated gases were as follows: 500 ppm of NO, 500 ppm of NH_3, 6.1% of O_2, 6.4% of H_2O and balanced with N_2. The total flow rate was 320 mL/min, and the corresponding gas hourly

Table 1
Detailed hydration procedures in this study.

Method	Step 1	Step 2	Step 3	Step 4	Step 5	Step 6
1	20 min under dry air flow (180 mL/min) at 600 °C	Cooled down to 80 °C without gas flow	Catalyst was aged in moisture flow (253 mL/min, 10% H_2O/N_2) at 80 °C for desired time	Heated up to 600 °C and hold for 20 min in dry airflow	Cooled down to 150 °C in reactant gas	Activity test
2			Catalyst was aged in moisture flow (253 mL/min, 10% H_2O/N_2) at 80 °C for 30 min		Moved to step 2 to start next cycle or cooled down to 150 °C in reactant gas	

[1]Hydration time method; [2]Cycle hydration method.

space velocity (GHSV) was 300,000 h^{-1}. The concentrations of NO_x (NO and NO_2) and N_2O in the inlet and outlet gases were continually analyzed by a Fourier transform infrared (FTIR) spectrometer (Tensor 27, Bruker) with a 2 m gas cell. All catalysts were pretreated in the simulated gases at 550 °C for 2 h before activity test. Catalytic activity tests were carried out over the temperature range of 150 to 500 °C, and activity results were recorded after holding at each temperature for 40 min. The NO_x conversion was calculated by using the following formula:

$$NO_x\ \text{conversion}\,(\%) = \frac{([NO]_{in} - [NO]_{out} - [NO_2]_{out} - 2[N_2O]_{out}}{[NO]_{in}} \times 100\% \quad (1)$$

2.3. Kinetic test

The kinetic test was performed by 16.5 mg of pellets Cu-SAPO-34 catalyst (60–80 mesh) mixed with 300 mg of quartz beads (60–80 mesh) in a fixed bed quartz flow reactor as reported above, The concentrations of the simulated gases were as follows: 500 ppm of NO, 500 ppm of NH_3, 6.1% of O_2, 6.4% of H_2O and balanced with N_2. The total flow rate was 900 mL/min, and the GHSV was 3,270,000 h^{-1}. All catalysts were pretreated in the simulated gases at 550 °C for 2 h before test. Catalytic activity tests were carried out over the temperature range of 150–300 °C, and activity results were recorded after holding at each temperature for 40 min. The TOF was calculated by using the following formula:

$$TOF = \frac{NO\ \text{conversion}\,(\%) \times F \times [C] \times 63.5}{22.4 \times m \times w} (s^{-1}) \quad (2)$$

Here, F is total flow rate, [C] is the concentration of inlet NO_x, m is the mass of catalyst and w is mass percentage of isolated-Cu^{2+} ions (determined by EPR) on Cu-SAPO-34.

2.4. Catalyst characterization

An automatic surface analyzer system (Micromeritics ASAP 2020) was used to measure the N_2 adsorption isotherms of the samples at the temperature of liquid N_2 (−196 °C). The specific surface areas were determined from the linear portion of the BET plot. Prior to the adsorption of N_2, all samples were evacuated at 350 °C for 6 h.

The chemical content of each sample was determined by X-ray fluorescence (XRF, Axios advanced, PANalytical).

XRD data were collected on X'Pert Pro diffractometer (PANalytical) with Cu radiation (λ = 0.15406 nm). The X-ray tube was operated at 40 kV and 40 mA. The samples were investigated in the 2θ range of 5–50° at a scanning speed of 0.02°/s. The relative crystallinity was calculated based on the formula:

$$R = \frac{\text{Sum of three strongest peaks of sample}}{\text{Sum of three strongest peaks of sample C}} \times 100\% \quad (3)$$

All the solid state NMR experiments were performed using a Varian Infinity-plus 400 spectrometer equipped with a 9.4 T wide-bore magnet. The resonance frequencies were 79.4 MHz, 156.4 and 242.9 MHz for ^{29}Si, ^{27}Al and ^{31}P, respectively. ^{29}Si MAS NMR experiments were performed using a 5 mm MAS probe with a spinning rate of 8 kHz. ^{27}Al and ^{31}P MAS NMR experiments were performed using a 4 mm MAS probe with a spinning rate of 12 kHz. ^{29}Si MAS NMR spectra were recorded using high power proton decoupling sequence. 1024–3072 scans were accumulated with a π/4 pulse width of 2.5 μs and a 10 s recycle delay. Chemical shifts were referenced to kaolinite at −91.5 ppm. ^{27}Al MAS NMR spectrum was recorded using a one pulse sequence. 200 scans were accumulated with a π/8 pulse width of 0.75 μs and a 2 s recycle delay. Chemical shifts were referenced to $(NH_4)Al(SO_4)_2{\cdot}2H_2O$ at −0.4 ppm. ^{31}P MAS NMR spectrum was recorded using high-power proton decoupling. 32 scans were accumulated with a π/4 pulse width of 2.25 μs and a 10 s recycle delay. Chemical shifts were referenced to 85% H_3PO_4 at 0 ppm.

EPR spectra were performed on Bruker A 200 at 102 K. The sample was pre-treated in dry air at 500 °C for 4 h, then cooled down to 120 °C in dry air. Finally, the sample was treated in pure N_2 at 120 °C for 24 h before test. During spectral collection, microwave power was 2.007 mW and frequency was 9.51 GHz. The sweep width was 2000 G and sweep time was 83.968 s, modulated at 100 kHz with a 2 G amplitude. A time constant of 40.960 ms was used. Standard $CuSO_4$ solution was used to quantify the content of isolated Cu^{2+} ions in the Cu-SAPO-34 catalyst.

The H_2-TPR was conducted on a chemisorption analyzer with a TCD detector (Micromeritics, AutoChem II). 80 mg of sample was first pretreated in Ar (30 mL/min) at 500 °C for 1 h to remove the H_2O and other impurities adsorbed on the surface of sample. Then, the sample was cooled down to 100 °C in Ar flow, the H_2-TPR was carried out at a linear heating rate of 10 °C/min from 100 to 700 °C under 10 vol% H_2/Ar (30 mL/min) flow.

NH_3-TPD was carried out on chemisorption analyzer (Micromeritics, AutoChem II). 100 mg of sample was first pretreated in He (30 mL/min) at 500 °C for 1 h to remove the H_2O and other impurities in the sample. Then, the sample was cooled down to 120 °C and exposed in NH_3 (2% NH_3/He, 30 mL/min) for 30 min, after that the catalyst was purged by He (30 mL/min) for 60 min to remove physically adsorbed NH_3. The measurement of the desorbed NH_3 was performed from 120 to 600 °C (10 °C/min) under He flow (30 mL/min).

3. Results and discussion

3.1. Activity test

Although the negative effect of low-temperature vapor on the stability of Cu-SAPO-34 catalyst has been recognized, the influence of hydration temperature is still unclear so far. Herein, we first investigate the effect of hydration temperatures (40–120 °C) and the results are shown in Fig. A1. Clearly, with the increase of the hydration treatment temperature from 40 to 80 °C, a gradual activity drop can be observed for the corresponding treated catalysts. The deactivation trend starts to be relieved after increasing the hydration temperature to 100 °C. Further increasing to 120 °C, little activity variation can be observed as compared with that of the fresh one. The results imply that hydration treatment at 80 °C is the harshest condition resulting in the most severe activity decay of Cu-SAPO-34 catalyst. Hence, 80 °C is selected as the

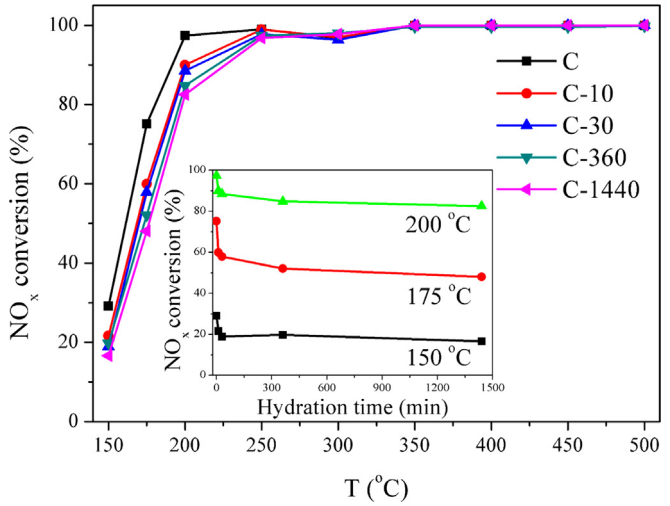

Fig. 1. NH_3-SCR activities of Cu-SAPO-34 catalysts before and after low-temperature hydration treatment. Aging condition is the method 1 in Table 1. GHSV: 300,000 h^{-1}.

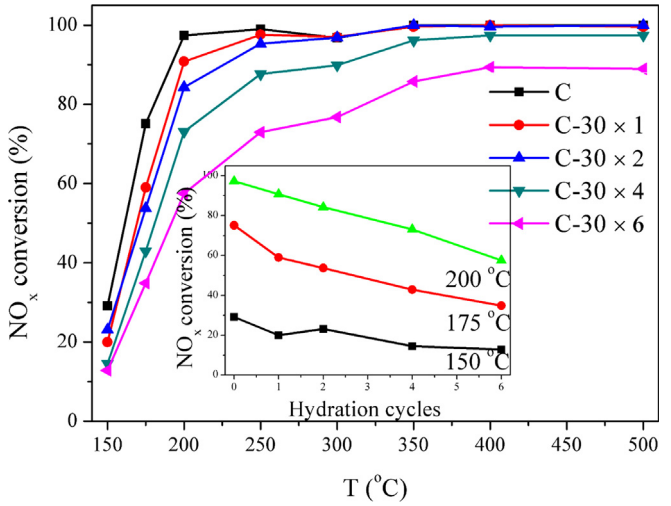

Fig. 2. NH_3-SCR activities of Cu-SAPO-34 catalysts before and after multiple-cycle hydration. Aging condition is described by the method 2 in Table 1. GHSV: 300,000 h^{-1}.

standard hydration temperature to test the impact of hydration time and cycles on the NH_3-SCR activity of Cu-SAPO-34 catalyst.

3.1.1. The effect of hydration time method on the NH_3-SCR performance of Cu-SAPO-34 catalyst

Fig. 1 shows the reaction results of the catalysts after hydration treatment at 80 °C for 0, 10, 30, 360 and 1440 min, respectively. It can be seen that the NH_3-SCR activities of Cu-SAPO-34 catalysts in the low-temperature region decline with the extension of hydration time. To better display the activity change with the hydration time, NO_x conversion (at 150, 175 and 200 °C) as a function of hydration time is plotted and given in the inset of Fig. 1. Clearly, the most obvious activity decline occurs at the initial hydration stage of 30 min. Afterwards, the decreasing rate of NO_x conversion slows down until 1440 min.

3.1.2. The effect of cycle hydration method on the NH_3-SCR performance of Cu-SAPO-34 catalyst

Cycle hydration experiments are designed to determine the influence of multiple hydration treatment on the SCR activity of Cu-SAPO-34 catalyst. In one treatment cycle, the catalyst was first exposed to the vapor at 80 °C for 30 min and then heated up to 600 °C under dry air to exclude the negative effect of adsorbed H_2O molecule. Afterward, the catalyst was cooled down to 80 °C to start another cycle or activity test (Table 1). The catalytic results on Cu-SAPO-34 catalysts before and after cycle hydration are shown in Fig. 2. It can be found that the NH_3-SCR activities on Cu-SAPO-34 catalysts obviously decrease with the increase of the hydration cycles. The NO_x conversion (at 150, 175 and 200 °C) is plotted as a function of hydration cycles and presented in the inset of Fig. 2. Clearly, the NO_x conversion at 175 or 200 °C drops in a quasi-linear manner with the increase of the hydration cycles. In order to exclude the possible influence of repeated 600 °C treatment on the NH_3-SCR performance of Cu-SAPO-34 catalyst, contrast experiments (repeated thermal treatment at 600 °C without low-temperature hydration) were carried out. As shown in Fig. A2, the NH_3-SCR activities of all the Cu-SAPO-34 catalysts are almost identical, confirming that the deteriorated catalytic performance of Cu-SAPO-34 catalyst is caused by the low-temperature hydration treatment. On the other hand, the N_2 selectivity during the NH_3-SCR process over Cu-SAPO-34 catalysts before and after low-temperature hydration is very high (> 99%) and changes little (Fig. A3), suggesting that hydration treatment does not affect the N_2 selectivity.

It is interesting to note that although the total hydration time of C-30 × 6 catalyst (180 min) is shorter than that of C-1440 catalyst (1440 min), the NH_3-SCR activities of the former catalyst are evidently worse than those of the latter one, showing that cycle hydration method causes more severe damage on the catalytic performance. The results imply that cycle hydration treatment should be a more effective method to evaluate the low-temperature hydrothermal stability of Cu-SAPO-34 catalyst.

3.2. Textural and structural properties

The textural properties of the catalysts before and after low-temperature hydration treatment were measured, and the results are summarized in Table 2. The surface areas and pore volumes of Cu-SAPO-34 catalyst show a slight decrease after low-temperature hydration treatment. However, the difference among the treated catalysts is small and no regular variation tendency can be observed, implying that the low-temperature hydration treatment has little effect on the textural properties of the SAPO-34 support under the present conditions. All the XRD patterns present diffraction peaks typical of SAPO-34 structure (Fig. A4). From Table 2, the relative crystallinity (R) of some samples is even higher than that of the fresh one, confirming that the low-temperature hydration treatment does not damage the integrity of structure. Therefore, the evident loss of NH_3-SCR activity of the treated Cu-SAPO-34 catalysts should not be due to the crystallinity change of the catalyst.

Table 2
Textual and structural properties of Cu-SAPO-34 catalyst before and after low-temperature hydration treatment.

Sample	S_{BET} (m^2/g)[1]	S_{micro} (m^2/g)[2]	V_{total} (mL/g)[3]	V_{micro} (mL/g)[4]	R(%)[5]
C	702	683	0.29	0.27	100
C-30	618	615	0.25	0.25	118
C-360	646	660	0.26	0.27	97
C-1440	625	621	0.25	0.25	119
C-30 × 2	688	672	0.27	0.27	121
C-30 × 4	627	624	0.26	0.25	119
C-30 × 6	650	636	0.26	0.25	97

[1] BET surface area.
[2] S_{micro} (micropore area).
[3] Adsorbed volume at $P/P_0 = 0.98$.
[4] V_{micro} (micropore volume) are determined by the t-plot method.
[5] Relative crystallinity.

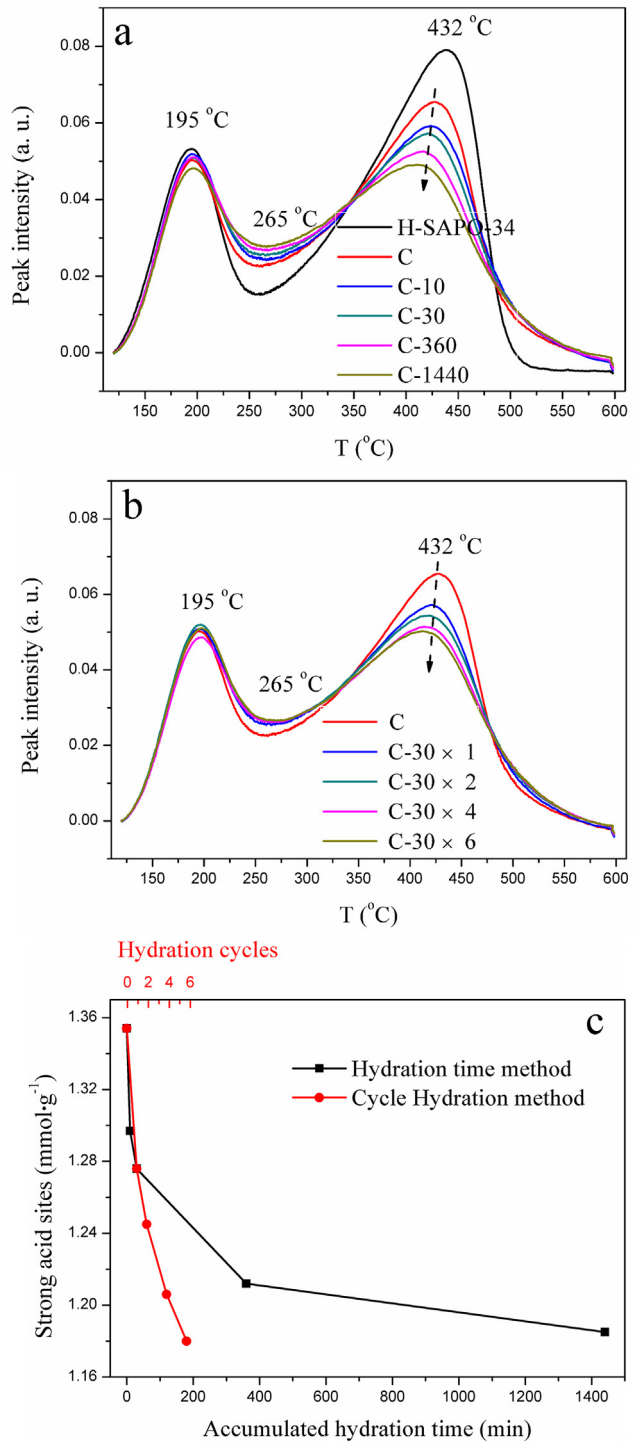

Fig. 3. NH_3-TPD profiles of Cu-SAPO-34 catalysts before and after different hydration time (a) and hydration cycles (b). The change trend of strong acid sites as the accumulated hydration time (c). The strong acid sites were calculated on the basis of the peak area in the temperature range of 300–600 °C in the NH_3-TPD profiles.

3.3. Acid property

The acid properties of Cu-SAPO-34 catalyst are important to the NH_3-SCR activity. Yu *et al.* demonstrated that the Cu-SAPO-34 catalyst with higher acid density was beneficial for the NH_3-SCR activity [20]. Wang et al. recently revealed that the Cu-SAPO-34 catalyst with larger amount of strong structural Brönsted acid sites possessed better NH_3-SCR performance [21]. Herein, NH_3-TPD experiments were conducted to probe the acid properties of the catalysts. From Fig. 3, the profiles of all the samples contain two distinguishable regions, which can be deconvoluted into three peaks located at ca. 195, 265 and 432 °C, respectively. According to the literatures, for H-SAPO-34, the peak at 195 °C is attributed to weakly bounded NH_3 [22], which includes the contributions of physisorbed NH_3 and NH_3 adsorbed on surface hydroxyls (P-OH or Al-OH) [23,24]; the peaks at higher temperatures (265 and 432 °C) are related with the Brönsted acid sites of moderate and strong acid strength, respectively [24]. Given that the fresh Cu-SAPO-34 sample shows an increased peak at 265 °C at the expense of the peak at 432 °C as compared with H-SAPO-34, it is speculated that the incorporated Cu^{2+} ions occupy part of strong Brönsted acid sites, provide additional Lewis acid sites and contribute to the increase of medium-temperature peak [25]. In addition, the peak at 432 °C in the NH_3-TPD profile of Cu-SAPO-34 may also include the contribution of strong Lewis acid sites aroused by Cu^{2+} ions [23].

For the catalysts treated by hydration time method, the peak at 195 °C keeps almost unchanged with the increase of hydration time. Meanwhile, the peak at 265 °C shows a slight rise and the peak at 432 °C gradually decreases. Since the content of isolated Cu^{2+} ions (corresponding to Lewis acid sites) is almost unchanged (see the following EPR section, the change of isolated Cu^{2+} ions on C-30 is only 0.007 $mmol \cdot g^{-1}$, which is much lower than the variation of strong acid sites), these variations imply a gradual loss of the Brönsted acid sites, evidencing that the structural Si-OH-Al bonds are sensitive to the low-temperature vapor [13]. The catalysts undergo cycle hydration also show a similar trend.

To better compare the variation of the acid sites in the two sets of catalysts, the content of strong acid sites is plotted as a function of the accumulated hydration time (Fig. 3c). For Cu-SAPO-34 catalysts treated by hydration time method, the strong acid sites diminish quickly at the initial stage of 30 min. Afterwards, the dropping rate slows down with time until 1400 min. For Cu-SAPO-34 catalysts treated by cycle hydration method, the strong acid sites show a quasi-linear decrease with the total hydration time and the dropping rate is obviously faster than that of the former set of catalysts. The decrease trend of the strong acid sites is consistent with the deterioration of the NH_3-SCR performance of Cu-SAPO-34 catalysts, indicating that the close relevance of the strong acid sites and the activity. On the other hand, given that samples having similar acid sites (e.g. C-30 × 6 vs. C1440) behave distinct NH_3-SCR activity, we speculated that besides acidity, other properties which are important to the NH_3-SCR reaction, might also be altered during the low-temperature hydration treatment.

3.4. ^{29}Si MAS NMR

The Brönsted acid sites of SAPO-34 are generated due to the introduction of Si atoms into the neutral $AlPO_4$-34 framework [26]. And the variation of Si coordination environments in SAPO-34 would affect its acidity. Hence, ^{29}Si MAS NMR was used to probe the change of Si species before and after low-temperature hydration treatment (Fig. 4). No defect Si species can be found in Fig. 4, as well as defect P and Al species in Fig. A6, indicating that the structural integrity of SAPO-34 keeps well after hydration treatment. The de-convoluted processes of different Si species are shown in Fig. A5 and the corresponding quantitative results are listed in Table 3. Clearly, with the increase of hydration time or cycles, the content of Si islands rises at the expense of Si $(OAl)_4$ species, suggesting a gradual transformation of $Si(OAl)_4$ species to Si islands induced by low-temperature vapor. This change agrees with the decreased strong acid concentration of the treated catalysts as revealed by NH_3-TPD, since the average Brönsted acid sites per Si atom in the Si islands (< 1) is lower than that of $Si(OAl)_4$ species ($= 1$)[27].

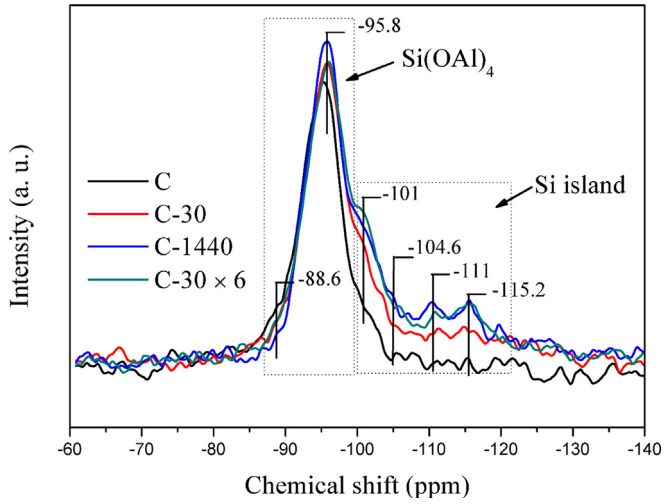

Fig. 4. ^{29}Si MAS NMR spectra of Cu-SAPO-34 catalysts before and after low-temperature hydration treatment.

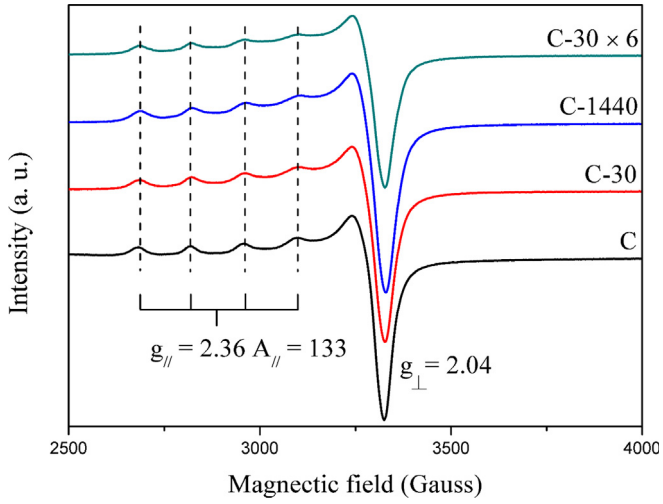

Fig. 5. EPR spectra of Cu-SAPO-34 catalysts before and after low-temperature hydration treatment.

Table 3
The de-convoluted results of different Si species based on the ^{29}Si MAS NMR spectra of the samples.

Sample	The proportion of various Si species (%)					
			Si islands			
	d-Si(OAl)$_4$[1]	Si(OAl)$_4$[2]	Si(OAl)$_3$[3]	Si(OAl)$_2$[4]	Si(OAl)$_1$[5]	Si(OAl)$_0$[6]
C	5.4	88.8	4.8	0.4	0.3	0.4
C-30	1.4	81.1	8.9	2.3	2.9	3.4
C-360	1.5	77.7	8.7	3.4	3.1	5.6
C-1440	0.3	71	9.8	5.2	6.2	7.5
C-30×2	7.2	79.7	8.9	0.8	1.2	2.2
C-30×4	3.6	73.7	8.7	1.4	5.5	7
C-30×6	1	71	9.5	5.4	5.2	7.8

[1]Disordered-Si(OAl)$_4$ at −88.6 ppm. [2]−95.8 ppm. [3]−101 ppm. [4]−104.6 ppm. [5]−111 ppm. [6]−115.2 ppm.

3.5. The effect of low-temperature hydration treatment on the active sites of Cu-SAPO-34 catalyst

3.5.1. Location and content of isolated Cu^{2+} ions

EPR is an efficient method to characterize the content and location of isolated Cu^{2+} ions, since it is only responsive to isolated Cu^{2+} ions and silent to other Cu species (CuO, $[Cu\text{-}O\text{-}Cu]^{2+}$, O-Cu-O and Cu^{+}) [16]. As displayed in Fig. 5, the EPR spectra of all catalysts show only one parallel g-value ($g_{//} = 2.36$) due to the isolated Cu^{2+} ions locate at six-membered ring sites (Site I) [28], indicating that the location of isolated Cu^{2+} ions is unchanged. The quantitative results from EPR spectra of the catalysts are shown in Fig. 6. It is clear that most of Cu species in the fresh Cu-SAPO-34 catalyst exist as isolated Cu^{2+} ions (0.98 wt%, amounting to 86% of the total Cu loading). Low-temperature hydration treatment has little influence on the content of isolated Cu^{2+} ions except for a relatively large change on catalyst C-30×6 with a 9% drop.

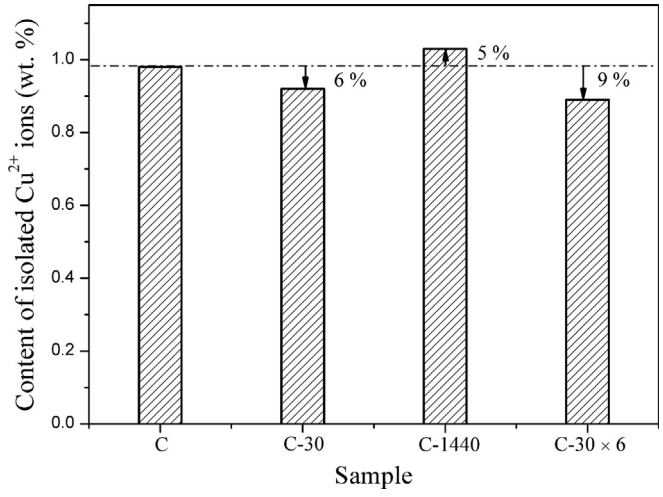

Fig. 6. The content of isolated Cu^{2+} ions in Cu-SAPO-34 catalysts before and after low-temperature hydration treatment.

3.5.2. Reducibility of copper species

H_2-TPR experiments were conducted to assess the reducibility of the Cu-SAPO-34 catalysts before and after hydration treatment, and the results are given in Fig. 7. All the profiles of Cu-SAPO-34 catalysts contain three reduction peaks that located at ca. 250, 390 and 590 °C, respectively. The first two peaks, correspond to the sequential reduction of isolated Cu^{2+} to Cu^{+} ions and Cu^{+} ions to Cu^{0} [29,30], while the third peak at 590 °C is attributed to the reduction of isolated Cu^{+} ions that are more difficult to be reduced [29,31].

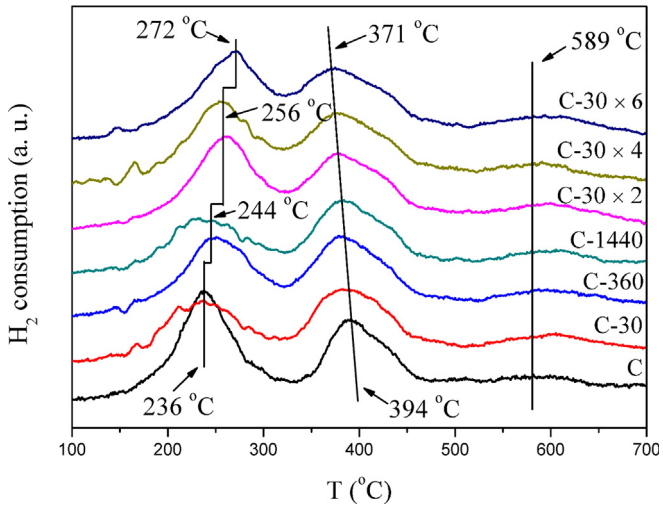

Fig. 7. H_2-TPR profiles of Cu-SAPO-34 catalysts before and after low-temperature hydration treatment.

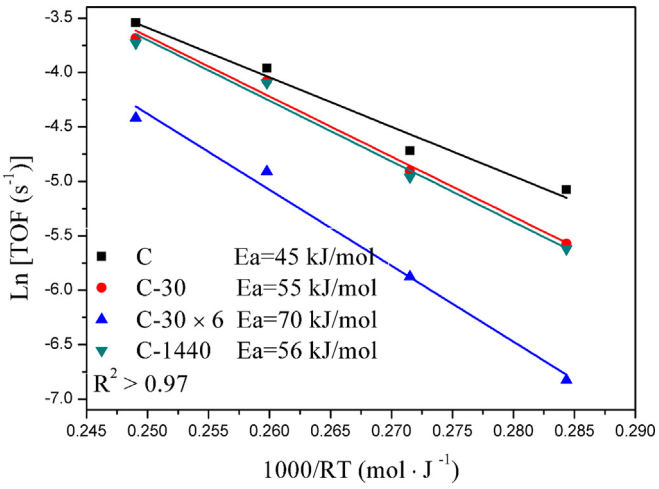

Fig. 8. Kinetic results of Cu-SAPO-34 catalysts before and after hydration treatment. GHSV: 3,270,000 h^{-1}.

Kispersky *et al.* reported that the NH_3-SCR reaction over Cu-SAPO-34 catalyst occurred via a redox cycle of Cu^+ and Cu^{2+} based on the results of *operando* XAS [32]. Paolucci et al. further investigated the reaction mechanism over Cu-CHA catalyst by *operando* XANES and DFT calculation [33], revealing that the Cu^{2+} species were reduced to Cu^+ by NO and NH_3, and Cu^+ species were oxidized by NO and O_2. Thus, the redox properties of Cu-SAPO-34 catalyst, namely the cycle between Cu^+ and Cu^{2+}, are very important to the NH_3-SCR activity. From Fig. 7, it can be found that the first peak of Cu-SAPO-34 gradually shifts to higher temperature with the prolonging of the hydration time. This trend becomes more evident for the catalysts surviving multiple cycle hydration. Similar trend can also be obtained from the Cu $2p_{3/2}$ XPS data displayed in Fig. A8 and Table A1. In contrast, the second reduction peak of Cu-SAPO-34 catalyst moves to lower temperature with the increase of hydration time or cycles, implying a decreased interaction between Cu species and SAPO-34 framework after low-temperature hydration treatment [31].

Martini et al. recently demonstrated that lower spatial proximity between Brönsted acid sites and Cu^{2+} complex in the CHA cages of SAPO-34 would result in a decreased reducibility of Cu^{2+} to Cu^+ by in-situ XAS and FTIR [34]. Herein, considering the decay of acid sites on the hydrated catalysts (evidenced by NH_3-TPD) and the change of Si coordination environments (revealed by ^{29}Si spectra), it is speculated that the chemical environments of Cu^{2+} ions (the interactions between the framework and Cu^{2+} ions) may be altered by the low-temperature hydration treatment, consequently leading to a decrease of the reducibility of Cu^{2+} to Cu^+. Possibly, the migration of Cu^{2+} ions from one cage (Site I) to another (Site I) occurs during the high-temperature dehydration intervals of cycle hydration treatment [35], which causes a deterioration of acid sites of the Cu-disappearing-region due to the lack of the protection of Cu^{2+} ions and thus the acid distribution changes. XPS was used to detect the surface elemental compositions of the catalysts. As shown in Table A1, an obvious drop of surface Cu and Si contents can be observed for catalyst C-30 × 6, which evidences the movement of Cu^{2+} ions and Si species in Cu-SAPO-34 and consists with our speculation about the variation of Cu reducibility and acidity.

It is thus supposed that the distinct difference between the two hydration methods results from the repeated high-temperature treatments involved in the cycle hydration, which prompt the migration of Cu^{2+} among the CHA cages. Because the Brönsted acid sites interacted with Cu^{2+} ions are more resistant to the hydrolyzation than the free ones [16], the movement of Cu^{2+} ions would fasten the loss of acid sites and alter the acid distributions in the catalyst crystals. Correspondingly, the isolated Cu^{2+} content, the micro-environments of Cu^{2+} ions and the reducibility of Cu^{2+} ions show a greater change after cycle hydration treatment than those treated by hydration time method.

3.6. Kinetic study

Kinetic tests were used to examine the TOF and apparent activation energy (Ea) over the catalysts before and after hydration treatment. As shown in Fig. A7, the influence of diffusion limitation of the reactants on the reaction rate can be eliminated under a GHSV of 3,270,000 h^{-1} and pellet diameter between 60 and 80 mesh. Fig. 8 shows the kinetic results of the catalysts. A gradual decrease of TOF can be observed following the order of C > C-30 > C-1440 > C-30 × 6. The Ea of catalyst C for NH_3-SCR in the temperature range between 150 and 210 °C is calculated to be 45 kJ/mol, which is similar to the values in the literatures [36,37]. After hydration treatment, the Ea of the catalysts shows an increase, suggesting that the activation barrier of NH_3-SCR increases. The variation of Ea is consistent with that of the TOF of the catalysts. For the catalysts C and C-30 having similar reducibility, C-30 with fewer strong acid sites shows higher value of Ea. On the other hand, for the catalysts C-30 × 6 and C-1440 with similar amount of strong acid sites, C-30 × 6 with lower reducibility of Cu^{2+} ions gives a higher value. These results evidence that both the decrease of strong acid sites and the decline of reducibility of Cu^{2+} to Cu^+ cause the increase of Ea value (corresponding to the activity deterioration of Cu-SAPO-34).

4. Conclusions

The impact of different low-temperature hydration conditions on the stability of Cu-SAPO-34 SCR catalysts have been explored through designed experiments. It is found that cycle hydration treatment on Cu-SAPO-34 causes a faster SCR activity deterioration than simply prolonging the hydration time. The characterization results demonstrate that insignificant difference exists in the surface areas, pore volumes, structure integrity of Cu-SAPO-34 catalysts before and after hydration treatment. The isolated Cu^{2+} ions are also less influenced by the low-temperature hydration treatment except a relatively large change on catalyst C-30 × 6 with a 9% drop. However, cycle hydration induces faster decay of the catalysts in strong acid sites and reducibility of Cu^{2+} to Cu^+ than hydration time method, which is in agreement with the change of their SCR activity. The high-temperature treatment process involved in the cycle hydration should be the main reason for the difference, which promotes the migration of Cu ions among the CHA cages and thus causes the decrease of Brönsted acid sites and the change of the micro-environments of Cu ions (the reducibility of Cu ions). Our present work also implies that cycle hydration treatment, which is close to the working conditions of the SCR catalyst, is an effective method to examine the low-temperature hydrothermal stability of the Cu-SAPO-34 catalysts.

Acknowledgement

We would like to thank the financial support from National Natural Science Foundation of China (No. 21473182, 91545104, 21606221 and 21676262), Key Research Program of Frontier Sciences, Chinese Academy of Sciences (Grant No. QYZDB-SSW-JSC040) and China Postdoctoral Science Foundation (Grant No. 2017M621169).

Appendix A. Supplementary data

Supplementary data associated with this article can be found, in the online version, at https://doi.org/10.1016/j.cej.2018.07.195.

References

[1] J. Wang, H. Zhao, G. Haller, Y. Li, Recent advances in the selective catalytic reduction of NO_x with NH_3 on Cu-Chabazite catalysts, Appl. Catal. B: Environ. 202

(2017) 346–354.
[2] L. Xie, F. Liu, L. Ren, X. Shi, F.S. Xiao, H. He, Excellent performance of one-pot synthesized Cu-SSZ-13 catalyst for the selective catalytic reduction of NO_x with NH_3, Environ. Sci. Technol. 48 (2013) 566–572.
[3] T. Johnson, Vehicular emissions in review, SAE Int. J. Engines 7 (2014) 1207–1227.
[4] P. Granger, V.I. Parvulescu, Catalytic NOx abatement systems for mobile sources: from three-way to lean burn after-treatment technologies, Chem. Rev. 111 (2011) 3155–3207.
[5] S.J. Schmieg, S.H. Oh, C.H. Kim, D.B. Brown, J.H. Lee, C.H.F. Peden, D.H. Kim, Thermal durability of Cu-CHA NH_3-SCR catalysts for diesel NO_x reduction, Catal. Today 184 (2012) 252–261.
[6] D.W. Fickel, E. D'Addio, J.A. Lauterbach, R.F. Lobo, The ammonia selective catalytic reduction activity of copper-exchanged small-pore zeolites, Appl. Catal. B: Environ. 102 (2011) 441–448.
[7] J.H. Kwak, D. Tran, S.D. Burton, J. Szanyi, J.H. Lee, C.H.F. Peden, Effects of hydrothermal aging on NH_3-SCR reaction over Cu/zeolites, J. Catal. 287 (2012) 203–209.
[8] Q. Ye, L. Wang, R.T. Yang, Activity, propene poisoning resistance and hydrothermal stability of copper exchanged chabazite-like zeolite catalysts for SCR of NO with ammonia in comparison to Cu/ZSM-5, Appl. Catal. A: Gen 427–428 (2012) 24–34.
[9] W. Su, H. Chang, Y. Peng, C. Zhang, J. Li, Reaction pathway investigation on the selective catalytic reduction of NO with NH_3 over Cu/SSZ-13 at low temperatures, Environ. Sci. Technol. 49 (2015) 467–473.
[10] W. Su, Z. Li, Y. Peng, J. Li, Correlation of the changes in the framework and active Cu sites for typical Cu/CHA zeolites (SSZ-13 and SAPO-34) during hydrothermal aging, Phys. Chem. Chem. Phys. 17 (2015) 29142–29149.
[11] L. Ma, Y. Cheng, G. Cavataio, R.W. McCabe, L. Fu, J. Li, Characterization of commercial Cu-SSZ-13 and Cu-SAPO-34 catalysts with hydrothermal treatment for NH_3-SCR of NO_x in diesel exhaust, Chem. Eng. J. 225 (2013) 323–330.
[12] D. Wang, Y. Jangjou, Y. Liu, M.K. Sharma, J. Luo, J. Li, K. Kamasamudram, W.S. Epling, A comparison of hydrothermal aging effects on NH_3-SCR of NO_x over Cu-SSZ-13 and Cu-SAPO-34 catalysts, Appl. Catal. B: Environ. 165 (2015) 438–445.
[13] M. Briend, R. Vomscheid, M.J. Peltre, P.P. Man, D. Barthomeuf, Influence of the choice of the template on the short- and long-term stability of SAPO-34 zeolite, J. Phys. Chem. 99 (1995) 8270–8276.
[14] A. Buchholz, W. Wang, A. Arnold, M. Xu, M. Hunger, Successive steps of hydration and dehydration of silicoaluminophosphates H-SAPO-34 and H-SAPO-37 investigated by in situ CF MAS NMR spectroscopy, Microporous Mesoporous Mater. 57 (2003) 157–168.
[15] K. Leistner, L. Olsson, Deactivation of Cu/SAPO-34 during low-temperature NH_3-SCR, Appl. Catal. B: Environ. 165 (2015) 192–199.
[16] J. Wang, D. Fan, T. Yu, J. Wang, T. Hao, X. Hu, M. Shen, W. Li, Improvement of low-temperature hydrothermal stability of Cu/SAPO-34 catalysts by Cu^{2+} species, J. Catal. 322 (2015) 84–90.
[17] C. Niu, X. Shi, K. Liu, Y. You, S. Wang, H. He, A novel one-pot synthesized CuCe-SAPO-34 catalyst with high NH_3-SCR activity and H_2O resistance, Catal. Commun. 81 (2016) 20–23.
[18] X. Xiang, P. Wu, Y. Cao, L. Cao, Q. Wang, S. Xu, P. Tian, Z. Liu, Investigation of low-temperature hydrothermal stability of Cu-SAPO-34 for selective catalytic reduction of NO_x with NH_3, Chin. J. Catal. 38 (2017) 918–927.
[19] X. Xiang, M. Yang, B. Gao, Y. Qiao, P. Tian, S. Xu, Z. Liu, Direct Cu^{2+} ion-exchanged into as-synthesized SAPO-34 and its catalytic application in the selective catalytic reduction of NO with NH_3, RSC Adv. 6 (2016) 12544–12552.
[20] T. Yu, J. Wang, M. Shen, W. Li, NH_3-SCR over Cu/SAPO-34 catalysts with various acid contents and low Cu loading, Catal. Sci. Technol. 3 (2013) 3234–3241.
[21] L. Wang, W. Li, S.J. Schmieg, D. Weng, Role of Brønsted acidity in NH_3 selective catalytic reduction reaction on Cu/SAPO-34 catalysts, J. Catal. 324 (2015) 98–106.
[22] Y. Qiao, P. Wu, X. Xiang, M. Yang, Q. Wang, P. Tian, Z. Liu, SAPO-34 synthesized with n-butylamine as a template and its catalytic application in the methanol amination reaction, Chin. J. Catal. 38 (2017) 574–582.
[23] D. Wang, L. Zhang, K. Kamasamudram, W.S. Epling, In situ-DRIFTS study of selective catalytic reduction of NO_x by NH_3 over Cu-exchanged SAPO-34, ACS Catal. 3 (2013) 871–881.
[24] J. Wang, T. Yu, X. Wang, G. Qi, J. Xue, M. Shen, W. Li, The influence of silicon on the catalytic properties of Cu/SAPO-34 for NOx reduction by ammonia-SCR, Appl. Catal. B: Environ. 127 (2012) 137–147.
[25] J.Y. Luo, F. Gao, K. Kamasamudram, N. Currier, C.H.F. Peden, A. Yezerets, New insights into Cu/SSZ-13 SCR catalyst acidity. Part I: Nature of acidic sites probed by NH3 titration, J. Catal. 348 (2017) 291–299.
[26] J. Tan, Z. Liu, X. Bao, X. Liu, X. Han, C. He, R. Zhai, Crystallization and Si incorporation mechanisms of SAPO-34, Microporous Mesoporous Mater. 53 (2002) 97–108.
[27] M. Zokaie, U. Olsbye, K.P. Lillerud, O. Swang, Stabilization of silicon islands in silicoaluminophosphates by proton redistribution, J. Phys. Chem. C 116 (2012) 7255–7259.
[28] A. Godiksen, F.N. Stappen, P.N.R. Vennestrøm, F. Giordanino, S.B. Rasmussen, L.F. Lundegaard, S. Mossin, Coordination environment of copper sites in Cu-CHA zeolite investigated by electron paramagnetic resonance, J. Phys. Chem. C 118 (2014) 23126–23138.
[29] J. Xue, X. Wang, G. Qi, J. Wang, M. Shen, W. Li, Characterization of copper species over Cu/SAPO-34 in selective catalytic reduction of NO_x with ammonia: relationships between active Cu sites and de-NO_x performance at low temperature, J. Catal. 297 (2013) 56–64.
[30] Y. Cao, S. Zou, L. Lan, Z. Yang, H. Xu, T. Lin, M. Gong, Y. Chen, Promotional effect of Ce on Cu-SAPO-34 monolith catalyst for selective catalytic reduction of NO_x with ammonia, J. Mol. Catal. A: Chem 398 (2015) 304–311.
[31] Y.J. Kim, J.K. Lee, K.M. Min, S.B. Hong, I.-S. Nam, B.K. Cho, Hydrothermal stability of CuSSZ13 for reducing NO_x by NH_3, J. Catal. 311 (2014) 447–457.
[32] V.F. Kispersky, A.J. Kropf, F.H. Ribeiro, J.T. Miller, Low absorption vitreous carbon reactors for operandoXAS: a case study on Cu/Zeolites for selective catalytic reduction of NO_x by NH_3, Phys. Chem. Chem. Phys. 14 (2012) 2229–2238.
[33] C. Paolucci, A.A. Verma, S.A. Bates, V.F. Kispersky, J.T. Miller, R. Gounder, W.N. Delgass, F.H. Ribeiro, W.F. Schneider, Isolation of the copper redox steps in the standard selective catalytic reduction on Cu-SSZ-13, Angew. Chem. 126 (2014) 12022–12027.
[34] A. Martini, E. Borfecchia, K.A. Lomachenko, I.A. Pankin, C. Negri, G. Berlier, P. Beato, H. Falsig, S. Bordiga, C. Lamberti, Composition-driven Cu-speciation and reducibility in Cu-CHA zeolite catalysts: a multivariate XAS/FTIR approach to complexity, Chem. Sci. 8 (2017) 6836–6851.
[35] P.N.R. Vennestrøm, A. Katerinopoulou, R.R. Tiruvalam, A. Kustov, P.G. Moses, P. Concepcion, A. Corma, Migration of Cu ions in SAPO-34 and its impact on selective catalytic reduction of NO_x with NH_3, ACS Catal. 3 (2013) 2158–2161.
[36] C. Niu, X. Shi, F. Liu, K. Liu, L. Xie, Y. You, H. He, High hydrothermal stability of Cu–SAPO-34 catalysts for the NH_3-SCR of NOx, Chem. Eng. J. 294 (2016) 254–263.
[37] X. Hu, M. Yang, D. Fan, G. Qi, J. Wang, J. Wang, T. Yu, W. Li, M. Shen, The role of pore diffusion in determining NH_3 SCR active sites over Cu/SAPO-34 catalysts, J. Catal. 341 (2016) 55–61.